communications earth & environment

ARTICLE

https://doi.org/10.1038/s43247-023-00981-5 OPEN

Taphonomy of non-biomineralized trilobite tissues preserved as calcite casts from the Ordovician Walcott-Rust Quarry, USA

Sarah R. Losso [1✉], Jennifer E. Thines[2] & Javier Ortega-Hernández [1✉]

Trilobites with appendages from the Rust Formation of New York State were discovered in the 1870s and represent one of the earliest known cases of exceptional preservation of non-biomineralized tissues. The Rust Formation trilobites feature three-dimensionally preserved walking legs and delicate respiratory lamellae, but the mechanism behind their fossilization remains unknown. Here we show that after burial, carcass decay produced framboidal pyrite, while fibrous calcite precipitated on the visceral side of the body, followed by the widespread formation of sparry calcite crystal replicating non-biomineralized morphological features. Trilobites and co-occurring calcite veins show no chemical or petrographic differences, rejecting the hypothesis that exceptional preservation was caused by a local microenvironment within enrolled trilobites. These results suggest that fine-grained sediment provided support for the appendages and facilitated their fossilization through calcite replacement. Our findings carry broader implications for understanding the exceptional three-dimensional preservation of animal Paleozoic body fossils through calcite casts.

[1] Museum of Comparative Zoology and Department of Organismic and Evolutionary Biology, Harvard University, Cambridge, MA 02138, USA. [2] Department of Geological Sciences, New Mexico State University, Las Cruces, NM 88003, USA. ✉email: sarahlosso@g.harvard.edu; jortegahernandez@fas.harvard.edu

The trilobites from the Walcott-Rust Quarry have been known for over 150 years[1–5] and represent an extremely rare case of exceptional three-dimensional preservation of non-biomineralized structures in the form of detailed biramous appendages fossilized as calcite casts within a micritic limestone (Fig. 1). Charles D. Walcott originally found and studied enrolled trilobite fossils in the 1870s, and further inspection of broken specimens led him to cut them into thin sections using steam-powered saws aided by his mother (Mary Walcott) and sister (Mary Josephine "Josie" Walcott)[6]. Preparing the specimens this way revealed exceptionally preserved three-dimensional appendages fossilized as calcite casts. Before this discovery, trilobite appendages had only been known from the endopodites (i.e., walking legs) of *Isotelus latus*[7], whereas the material from the Walcott-Rust Quarry produced the first ever insights into the biramous organization of the limbs including the lamellae-bearing exopodite[1–3].

The Rust Formation outcrops near Trenton Falls, New York, and is named for the family that owned the land when Charles D. Walcott opened a quarry there to collect trilobite fossils[6]. Exceptionally preserved specimens are only found within Layer 3 of the Spillway Member[5]. Body fossils within the Spillway Member of the Rust Formation were deposited in an obrution event, and include completely articulated trilobites in various positions (fully enrolled, partially enrolled, prone) within the layers or on the surface[5]. Two trilobites, *Flexicalymene senaria* Conrad 1841 and *Ceraurus pleurexanthemus* Green 1832 are commonly found within Layer 3 with exceptionally preserved appendages that include fine anatomical details such as delicate respiratory lamellae[5] (Fig. 1). Whereas the low-magnesium calcite exoskeletons of trilobites make them ubiquitous throughout the Paleozoic fossil record[8,9], their non-biomineralized appendages are much less frequently preserved. Given the rarity of trilobite appendages, only 40 species with known preserved appendages from an estimated diversity of 20,000 described species[10], understanding the taphonomic processes responsible for soft tissue fossilization in multiple well-preserved taxa in the same locality (e.g., *Ceraurus pleurexanthemus* and *Flexicalymene senaria* in Walcott-Rust) is critical for reconstructing their broader paleobiological significance and the conditions necessary for new discoveries. Despite being known for over a century, the morphology of the appendages of the two most common trilobites from the Walcott-Rust, *C. pleurexanthemus* and *F. senaria*, remains controversial. This is particularly true for fine anatomical details, such as the presence of endites[3,4,11], that are important for understanding the autecology and feeding strategy of trilobites[12].

Despite their iconic historical context, the Rust Formation trilobites have not been thoroughly studied in terms of their taphonomy. Previous work suggested that the exceptional fossils from the Walcott-Rust Quarry were produced by a process involving carcass decay through sulfate-reducing bacteria within a local microenvironment facilitated by the partially enrolled trilobites[5]. This model would require the production of bicarbonate and increase the pH within the isolated cavity formed by the

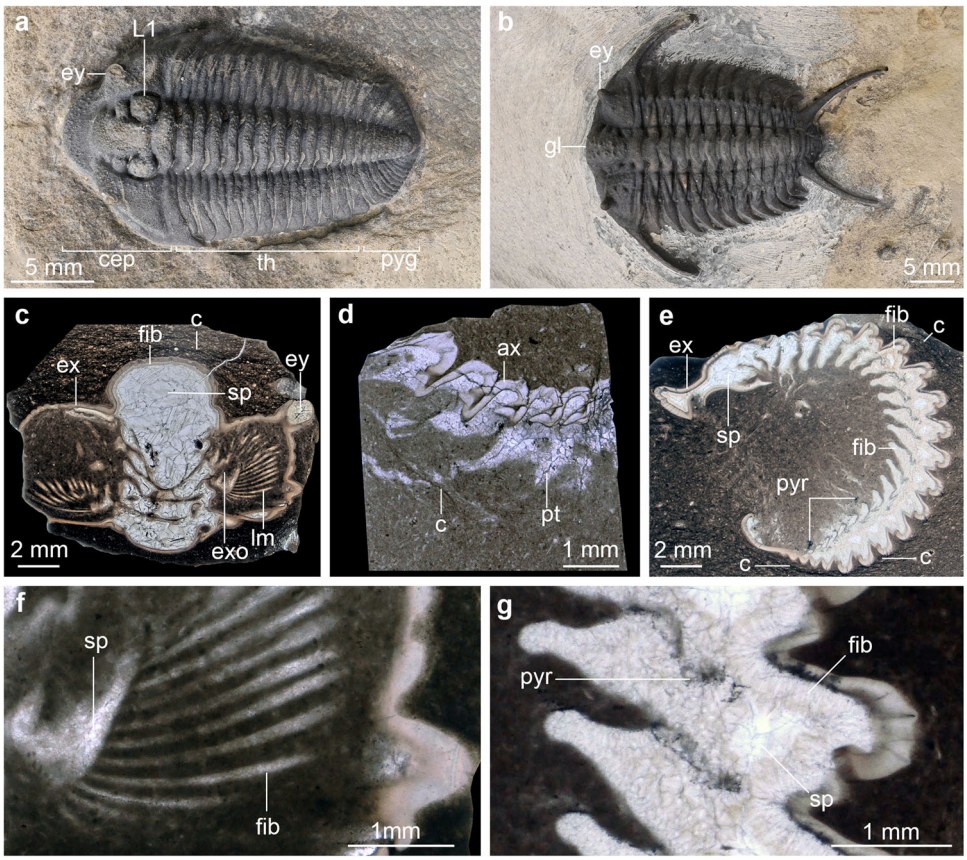

Fig. 1 Exceptionally preserved trilobites from the Walcott-Rust Quarry. a MCZ:IP:111710 prone *Flexicalymene senaria*. **b** MCZ:IP:111708 prone *Ceraurus pleurexanthemus*. **c** Photomicrograph of transverse thin section through cephalon of MCZ:IP:104973 with preserved exopodite and lamellae. **d** Photomicrograph of sagittal thin section along axial lobe of MCZ:IP:158215 with preserved protopodites. **e** Photomicrograph of sagittal thin section of MCZ:IP:104956 with preserved protopodites. **f** Magnification of exopodite of MCZ:IP:104973 showing calcite crystals within lamellae. **g** Magnification of protopodites in MCZ:IP:104956 showing pyrite, fibrous and sparry calcite. Abbreviations: ax, axial lobe; cep, cephalon; ey, eye; ex, exoskeleton; exo, exopodite; fib, fibrous calcite; gl, glabella; L1, lobe 1; pt, protopodite; pyg, pygidium; pyr, pyrite; sp, sparry calcite; th, thorax.

partially enrolled trilobites, leading to the precipitation of calcium carbonate that replicates the morphology of soft tissues[5]. Decay through sulfate-reducing bacteria would also play a key role in pyritization as it produces the sulfide which combines with iron[13]. Based on this parallel, previous authors[5] proposed that there was little available iron in the sediment as the carcass decayed, preventing complete pyritization and the pyrite seen in the specimens (Fig. 1e) replaced calcite later in diagenesis. Although this hypothesis for exceptional preservation in calcite has remain unchanged for over 20 years, its veracity has not been corroborated through chemical analyses, and thus the precise mechanism responsible for the formation of these fossils remains unclear. In this study, we take a comprehensive analytical approach through scanning electron microscopy, micro-computed tomography, and Raman spectroscopy on new and historic museum specimens to examine the phases of calcite precipitation, the formation of pyrite framboids, and the crucial role of sediment in appendage preservation in the Walcott-Rust trilobites.

Results

Exceptionally preserved trilobites from the Walcott-Rust Quarry show a consistent mineralogy that comprises an isopachous rim of fibrous calcite associated with framboidal pyrite that completely fills small void spaces, and large sparry calcite crystals in the larger spaces (Fig. 1c–e). Fully enrolled specimens with the pygidium tucked into the cephalon are filled with calcite (e.g., MCZ:IP:201000) and have no sediment matrix within the specimen (Fig. 2a, b). Sparry calcite infills most commonly occur within the glabella and doublure (Fig. 2c, f), which are surrounded by the biomineralized exoskeleton. Three specimens from Layer 8, higher in the stratigraphic column[5], have calcite infilling the doublure and glabella (Supplementary Fig. 2), but no appendages are visible in any of these fossils.

Pyrite occurs most commonly as framboids within the fossils and surrounding matrix (Fig. 3g, i). Fibrous calcite crystals form an isopachous rim ca. 150 µm long and grow inwards from the margin of the fossils (Fig. 1c, e–g). In small spaces, the fibrous crystals occupy the entire volume and are often colored with a faint orange hue that becomes more saturated towards the apex (Fig. 1e, g). Framboids are concentrated at the edges of fibrous crystals and frequently between the exoskeleton and the isopachous rim, but are also embedded within the crystals (Fig. 3g,) and seen throughout the matrix (Supplementary Figs. 3j, 4d). The sparry calcite crystals are clear, large, and blocky with the largest crystals near the center of the void space (Figs. 1c–g, 2a–c, f).

Fibrous crystals within veins are less well organized (Fig. 3h, j) as they nucleated off the uneven walls and grew inwards. Small syntaxial veins are filled by fibrous crystals with preserved median lines (Fig. 2c). In veins, pyrite framboids (Fig. 3i) fill large voids between fibrous or sparry crystals which are up to 1.5 mm long by 0.5 mm across (Fig. 3j). Comparisons indicate that trilobite fossils have noticeably less pyrite than veins, whereas the sparry calcite crystals are similar in appearance to those found in fossils and fill in larger spaces within veins (Fig. 3h, j).

Magnesium concentrations within the biomineralized calcitic exoskeleton vary from 1.2 wt% to concentrations below the limit of detection (<0.2 wt%; Fig. 4a, b; Supplementary Data 1). Fibrous and sparry crystals have overlapping ranges of magnesium, but compositions cluster based on specimens rather than crystal type (Fig. 4a, b). In MCZ:IP:198047, fibrous crystals have similar magnesium concentrations as the exoskeleton (Fig. 4a, b). Sparry crystals have decreasing magnesium towards the center of the calcite whereas most spots have non-detectable concentrations (Fig. 4a, Supplementary Data 1). The vein in MCZ:IP:199123 shows a similar pattern between fibrous and sparry crystals, although the concentrations are lower overall (Fig. 4a, b). Magnesium concentrations in sparry and fibrous calcite are similar within a single specimen but vary between specimens (Fig. 4a, b). The concentrations of calcium and carbon in the trilobite MCZ:IP:198048 and the vein MCZ:IP:199123 are similar and distinct from all other specimens (Fig. 4c). Iron concentrations are also consistent within specimens but vary between specimens. In MCZ:IP:198047, the sparry calcite has a higher iron concentration than the exoskeleton and fibrous calcite except for one spot (Fig. 4d, Supplementary Data 1, Supplementary Fig. 3). MCZ:IP:198048 has no detectable iron in the exoskeleton, fibrous, or sparry calcite. MCZ:IP:198046 has comparable values of iron in the sparry calcite as MCZ:IP:198047 (0.41–0.51 wt% and 0.41–0.59 wt%, respectively).

The matrix surrounding MCZ:IP:198047 shows dark rims around blocky clasts of feldspar which is high in iron with trace amounts of barium (0.29–0.71 wt%; Fig. 3b, Supplementary Data 1). The matrix within the specimen has a similar composition of clasts but lacks the dark rims and barium (Fig. 3d). Two fully enrolled specimens have large masses of barite within the body (Fig. 4e–i). In MCZ:IP:8400, barite (Fig. 4i) occupies a third of the internal volume, centered within the axial lobe with repeating lobe-like structures of uncertain origin (Fig. 4h). Compaction lines are frequently found surrounding fossils and are concentrated around opposite sides depending on the original orientation of the trilobite (Fig. 1c, e). Compaction lines are not seen within the sediment inside partially enrolled specimens or in the flexed specimen MCZ:IP:158215 (Fig. 1d).

Close morphological examination of trilobite thin sections demonstrates the presence of small spinose endites that extend from the medial and ventral edges of the protopodite, as well as from the distal edges of the podomeres on MCZ:IP:110933 and MCZ:IP:112018 (Fig. 5a–d). The base of the endites is comparable in width to the lamellae (ca. 0.1 mm), although they taper to a terminal width of 0.03 mm. Both endites and lamellae are filled with minute fibrous calcite crystals (Fig. 5a, b), and the crystals within the endites continue into the endopodite (Fig. 5b).

Discussion

Morphological identity of spinose endites in *Ceraurus pleurexanthemus*. The delicate quality of preservation of the Rust Formation trilobites includes fine morphological features (Fig. 1), but their appearance has caused some disagreement regarding their biological interpretation. For example, the spinose endites preserved on the ventral side of the limbs on *Ceraurus pleurexanthemus* have proven to be controversial (Fig. 5), with some authors regarding them as preservation artifacts[14] while others interpreted them as the true morphology[3]. Given the significance of endite morphology for reconstructing feeding strategies in trilobites[12], it is pertinent to clarify their nature to better understand the functional morphology of Ordovician species. Two specimens (MCZ:IP:110933 and MCZ:IP:112018) preserve a transverse cross section of *C. pleurexanthemus*, showing in detail the attachment side of the proximal region of the biramous appendages relative to the body wall (Fig. 5a–d). Here, examination of the walking legs demonstrate that the features interpreted as spinose endites are exclusively found on the ventral side of the protopodite and endopodite podomeres (Fig. 5a–d). The spinose projections are morphologically identical in both specimens and show a consistent perpendicular orientation relative to the main limb axis. Critically, there is no evidence of randomly oriented spinose projections on the dorsal side of the limbs or other parts of the body, which would be expected if these features resulted from taphonomic processes rather than reflecting the original anatomical organization. The placement of the spinose endites in

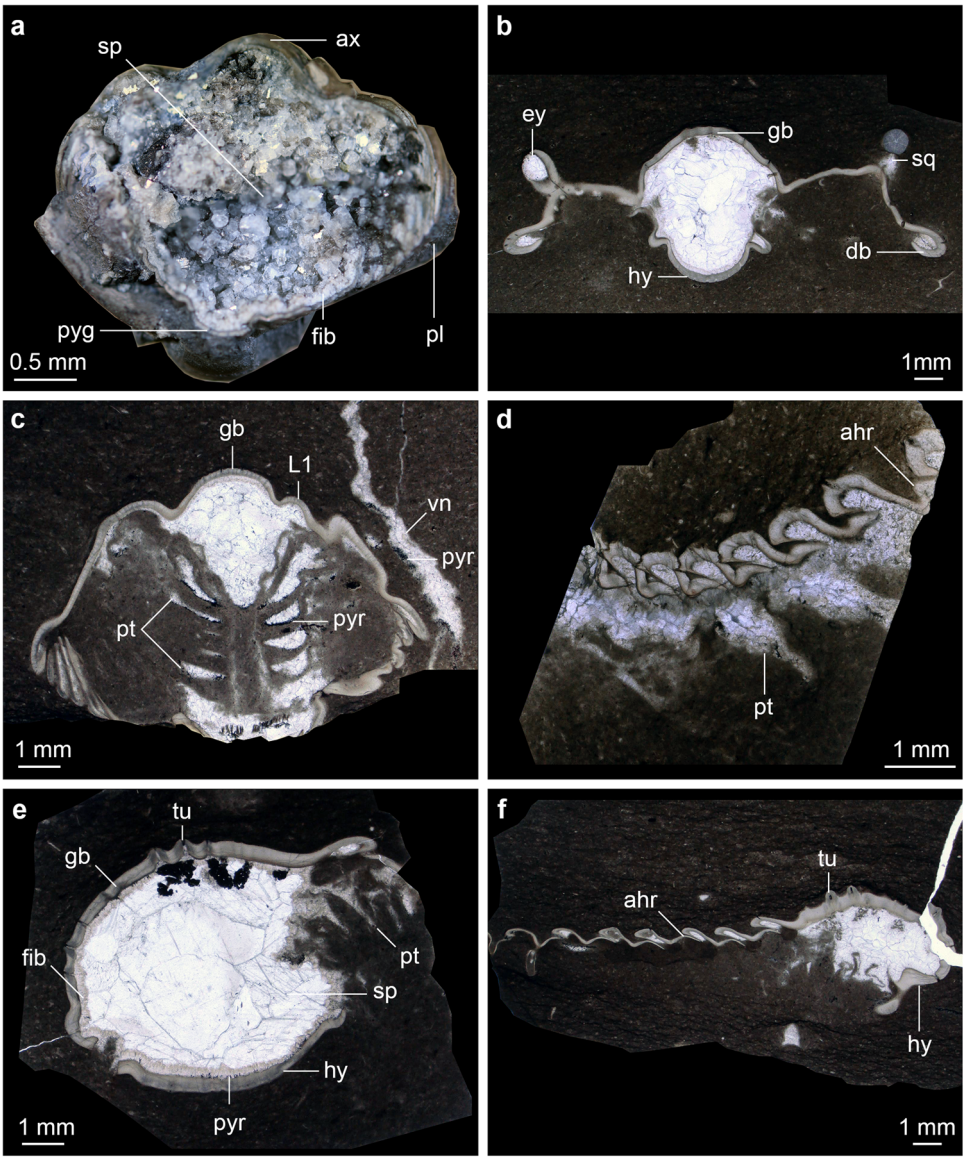

Fig. 2 Trilobites filled with calcite crystals from the Walcott-Rust Quarry Layer 3. a MCZ:IP:201000 from posterior view showing complete infilling of calcite crystals. **b** Photomicrograph of MCZ:IP:112022, a transverse thin section through the cephalon of *Ceraurus pleurexanthemus*. **c** Photomicrograph of MCZ:IP:110918, a transverse thin section through *Flexicalymene senaria* with a small vein filled by fibrous calcite. **d** Photomicrograph of MCZ:IP:158238, a sagittal thin section through *Ceraurus pleurexanthemus* in a flexed position with appendages. **e** Photomicrograph of MCZ:IP:112023, a sagittal thin section through *C. pleurexanthemus* showing calcite infill between glabella and hypostome. **f** Photomicrograph of MCZ:IP:112030, a sagittal thin section through *C. pleurexanthemus* showing calcite only between glabella and hypostome and within the axial rings. Abbreviations: ahr, articulating half ring; ax, axial lobe; ca, calcite; cep, cephalon; gb, glabella; hy, hypostome; L1, lobe 1; pl, pleural lobe; pt, protopodite; pyg, pygidium; tu, tubercle; vn, calcite vein.

MCZ:IP:110933 and MCZ:IP:112018 is extremely similar to that observed in other exceptionally preserved trilobites[10,15], including an arrangement along the medial and ventral edges of the protopodite, and clusters in the mid-point of podomeres or at the distal margin (Fig. 5). Direct comparisons with the protopodite and endopodite morphology of the Burgess Shale trilobite *Olenoides serratus* clearly exemplifies these similarities in terms of their overall appearance, location, and distribution (Fig. 5e–h). We conclude that the endites are not artifacts of preservation but reflect the original morphology of the Rust Formation trilobites. The morphological similarity of the protopodite outline and spinose endites observed between *C. pleurexanthemus* and *O. serratus* (Fig. 5) suggest that the former Ordovician species was incapable of a durophagous diet, and instead most likely feed on soft-bodied organisms and/or food items[12].

Effect of sediment and enrollment. The findings of this study suggest that the fine-grained sediment played an important role in supporting the delicate appendicular structures and facilitating exceptional preservation (Figs. 1, 2, 5). The limbs are not preserved in fully enrolled specimens in which sediment was not able to directly encase the appendages, and the resulting cavity formed by the exoskeleton is instead filled with sparry calcite (Figs. 2a, 6b). Calcite is commonly found between the glabella and the hypostome (Fig. 2b, c, e, f) as well as within the doublure (Fig. 3d), which share the fact that these locations are surrounded by the rigid exoskeleton. The exoskeleton created sheltered voids that were easily infilled by calcite crystals without requiring support from the sediment. Our interpretation is that fine-grained micritic limestone created a mold of even the most delicate structures (e.g., lamellae and endites) that was maintained as the carcass decayed. In cases in which

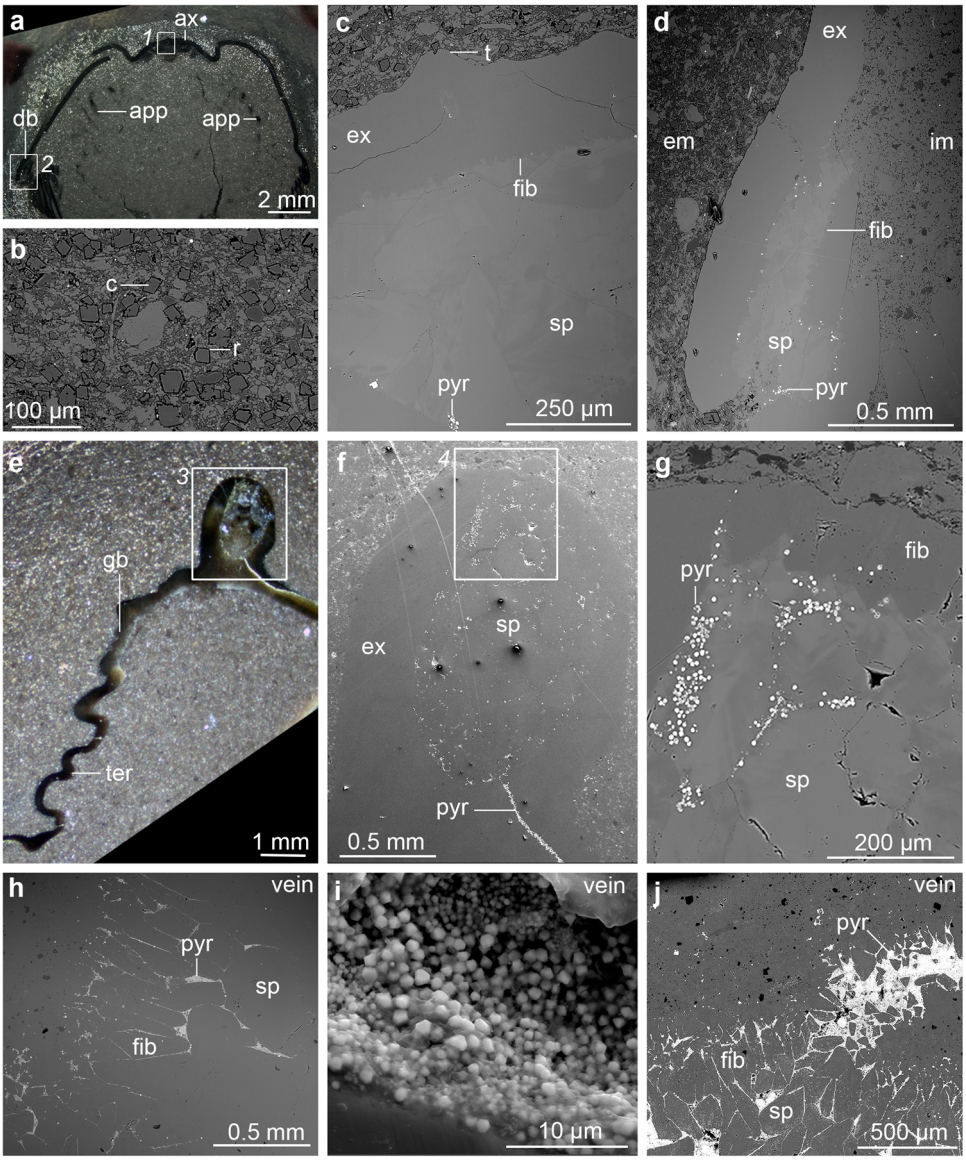

Fig. 3 Elemental and mineralogical comparison between trilobites and veins from the Walcott-Rust Quarry. a–d MCZ:IP:198047 *Flexicalymene senaria*. **a** Photomicrograph of polished surface in transverse cut through specimen showing appendage preservation. **b** Backscattered electron micrograph of matrix surrounding specimen. **c** Backscattered electron micrograph of axial lobe (box 1 in panel **a**) showing fibrous isopachous rim, sparry calcite and pyrite. **d** Backscattered electron micrograph of broken doublure (box 2 in panel **a**) showing internal and external matrix. **e–g** MCZ:IP:198046 *Ceraurus pleurexanthemus*. **e** Photomicrograph of polished surface exsagittally cut through eye. **f** Backscattered electron micrograph of eye (box 3 of panel **e**) showing line of framboidal pyrite along interior edge of exoskeleton. **g** Backscattered electron micrograph of eye (box 4 of panel **f**) showing fibrous calcite nucleated off lens, sparry calcite and pyrite. **h** Backscattered electron micrograph of calcite vein MCZ:IP:199124 showing poorly organized fibrous calcite, sparry calcite, and pyrite between crystals. **i** Backscattered electron micrograph of pyrite between crystals of H. **j** Backscattered electron micrograph of calcite vein MCZ:IP:199123 showing large amount of pyrite framboids within veins. Abbreviations: app, appendage; ax, axial lobe; c, clast; db, doublure; em, external matrix; ex, exoskeleton; fib, fibrous calcite; gb, glabella; im, internal matrix; sp, sparry calcite; t, tubercle; ter, tergite; r, barite rim around clast; pyr, pyrite.

the appendages were damaged during transport within the turbidity flow[16], the micritic mud mold was not able to form around the appendages, and thus calcite only formed within the exoskeleton-protected voids (Fig. 6c). Calcite is also found within the glabella and doublure of trilobites from Layer 8 which is higher in the section (Supplementary Fig. 2), but no appendages have been found from these specimens. Layer 8 is over twice as thick as Layer 3, and with the larger turbidity flow, the delicate appendages of trilobites may have been more prone to damage. When appendages were undamaged, the mud mold protected the external morphology of the limbs allowing for preservation of even the most delicate structures (Figs. 1c, 6d).

Enrollment has a complex effect on exceptional preservation in the Rust Formation. Previous authors[5] hypothesized that the partial enrollment created a microenvironment because of the protective barrier formed by the exoskeleton. Two specimens, MCZ:IP:158215 (Fig. 1d) and MCZ:IP:158238 (Fig. 2d), have preserved appendages, but critically these specimens are slightly dorsally flexed rather than enrolled. This indicates that enrollment was not a strict requirement for limb preservation. Evidence of compaction is commonly observed in the external sediment around the fossil (Fig. 1c, e), whereas there are no sediment compaction lines within the enrolled specimens. Interestingly, the protopodites of the prone specimen MCZ:IP:158215 (Fig. 1d) are

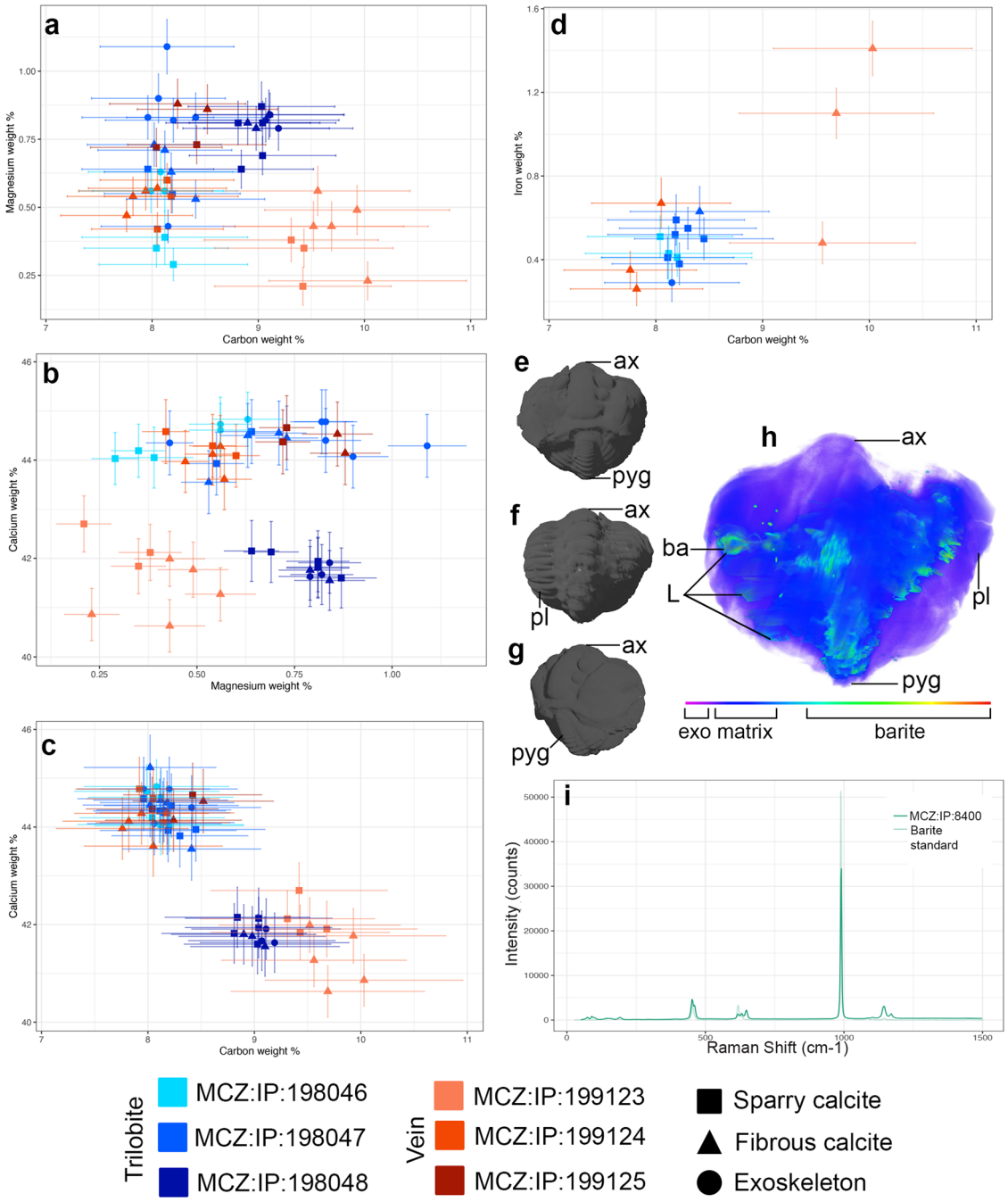

Fig. 4 Comparative chemical analyses of Rust Formation trilobites and veins. a–d Bivariate graphs of elemental weight percent from SEM spot analyses (see Supplementary Figs. 3–7) with error bars corresponding to 1 standard error (SE). **a** Carbon wt% versus magnesium wt%. **b** Magnesium wt% versus calcium wt%. **c** Carbon wt% versus calcium wt%. **d** Carbon wt% versus iron wt% for calcite in trilobites and veins. **e–g** Volume rendering of MCZ:IP:8400 showing external morphology. **h** Posterior view of volume rendering of MCZ:IP:8400 with dense barite mass (light green to red) inside following axial lobe and trunk tergites, blues and purples denote exoskeleton and matrix. Color scare denotes density differences with lower density material on the left colors and denser material on the right. **i** Raman spectroscopy of barite in MCZ:IP:8400 compared with barite standard. Abbreviations: ax, axial lobe; ba, barite; L, lobe like structure; pl, pleural lobe; pyg, pygidium.

not as well preserved as other specimens in a partially enrolled position, such as MCZ:IP:104956 (Fig. 1e), which suggests that the integrity of the mud mold around the appendages is important for their fossilization. Thus, although partial enrollment is not a prerequisite for appendage preservation, this position aided in the maintenance of the micritic mud mold and calcite cast during early diagenesis by decreasing the impact of compaction and resulting in a better preservation quality of ventral non-biomineralized structures. Such compaction could have distorted or damaged the appendages regardless of whether it occurred early or late during diagenesis.

No local microenvironment during decay. Our new data allows us to comprehensively test the traditional model for the exceptional preservation of soft tissues in the Rust Formation. Previous authors[5] proposed that partially enrolled trilobites from the Walcott-Rust Quarry created a microenvironment where calcite precipitation was induced within the cavity produced by the

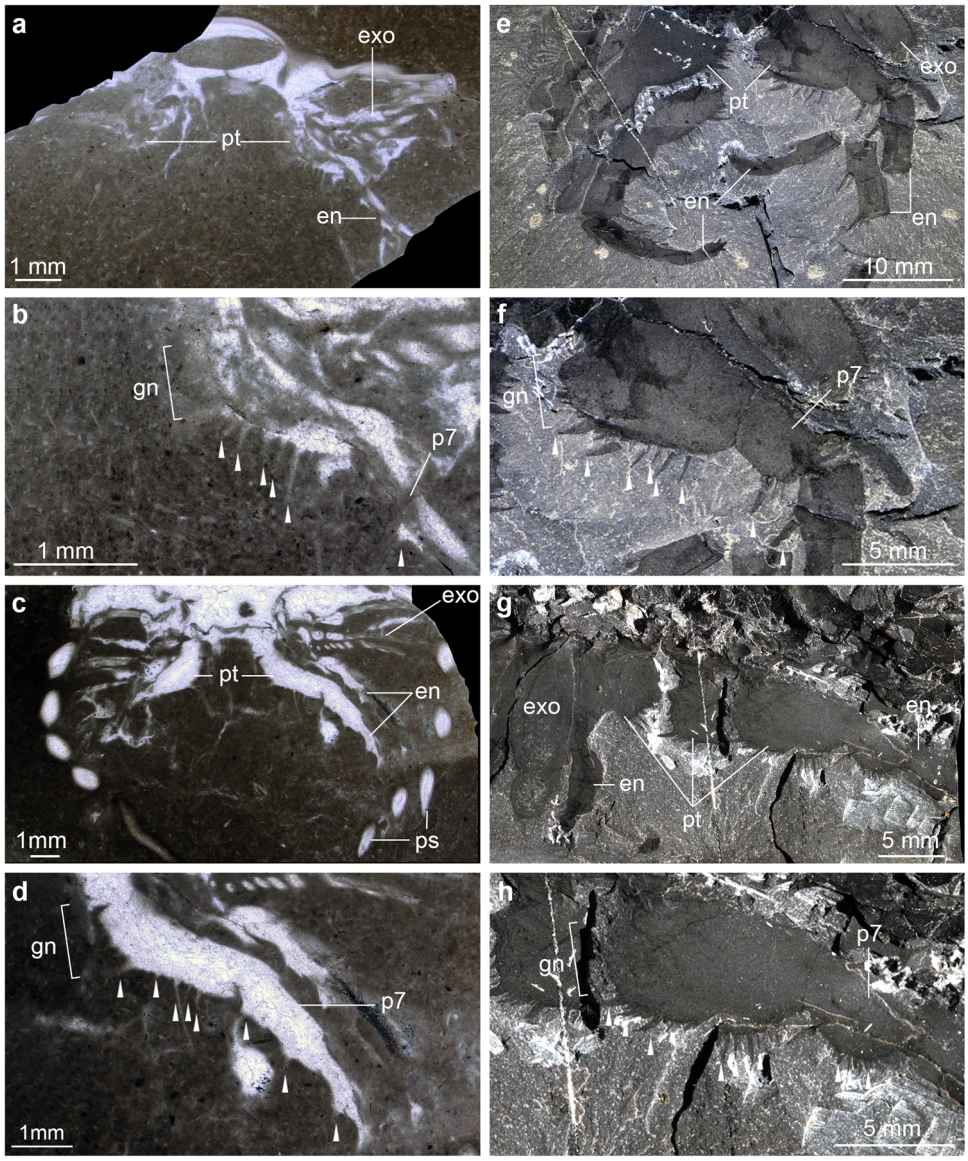

Fig. 5 Comparison of endites between *Ceraurus pleurexanthemus* and *Olenoides serratus* from the mid-Cambrian Burgess Shale. Arrow heads mark endites. **a** Photomicrograph of MCZ 110933, a transverse thin section through *C. pleurexanthemus* with a pair of preserved appendages. **b** Photomicrograph showing the proximal portion of the right appendage. **c** Photomicrograph of MCZ:IP:112018, a transverse thin section through *C. pleurexanthemus*. **d** Photomicrograph of MCZ:IP:112018 showing proximal portion of right appendage. **e** Dorsal view of *O. serratus*, GSC 34692. **f** Proximal portion of right appendage of GSC 34692. **g** Anterior view of *O. serratus*, USNM 65515. **h** Proximal portion of left appendage (image flipped horizontally to match orientation of panel **d**) of USNM 65515. Abbreviations; en, endopodite; exo, exopodite; gn, gnathobase; ps, pleural spine; p7, podomere seven; pt, protopodite.

specimen, and the exoskeleton acted as a physical protective barrier. Critically, this model would imply substantial physical and chemical discrepancies between the calcite formed within the trilobite fossil and the later-stage calcite veins found throughout the micritic rock matrix. However, we find no evidence of chemical differences between the calcite formed in fossils and veins, as both display the same crystal textures (i.e., a rim of fibrous crystals and large sparry crystals filling in larger voids) with no detectable differences in terms of elemental composition (Fig. 4). Four of the studied fossil specimens and veins (MCZ:IP:199124, MCZ:IP:199125, MCZ:IP:198046, MCZ:IP:198047) have similar calcite compositions, whereas two additional specimens (MCZ:IP:199123, MCZ:IP:198048) clustered together in terms of their magnesium and carbon content (Fig. 4b, c). Although MCZ:IP:199123 and MCZ:IP:198048 have similar values of calcium, MCZ:IP:198048 has higher magnesium, but both are within the range of the other veins and fossils (Fig. 4b). Original specimen locations within Layer 3 of the Rust Formation were not recorded during collection, so it is not clear if low-scale stratigraphic spatial distribution accounts for the similarities between MCZ:IP:199123 and MCZ:IP:198048. Although the calcite veins contain comparatively more pyrite than the trilobite fossils (Fig. 3j), both otherwise lack differences between composition and texture (Fig. 4c–e, h, j). Ultimately, we find no physical or chemical evidence for differences between the diagenetic formation of pyrite, fibrous calcite, and sparry calcite between trilobite body fossils, and the veins. We thus reject the hypothesis that enrolled trilobites produced a local microenvironment due to a barrier created by the exoskeleton that then facilitated exceptional preservation of soft tissues (*contra* previous authors[5]).

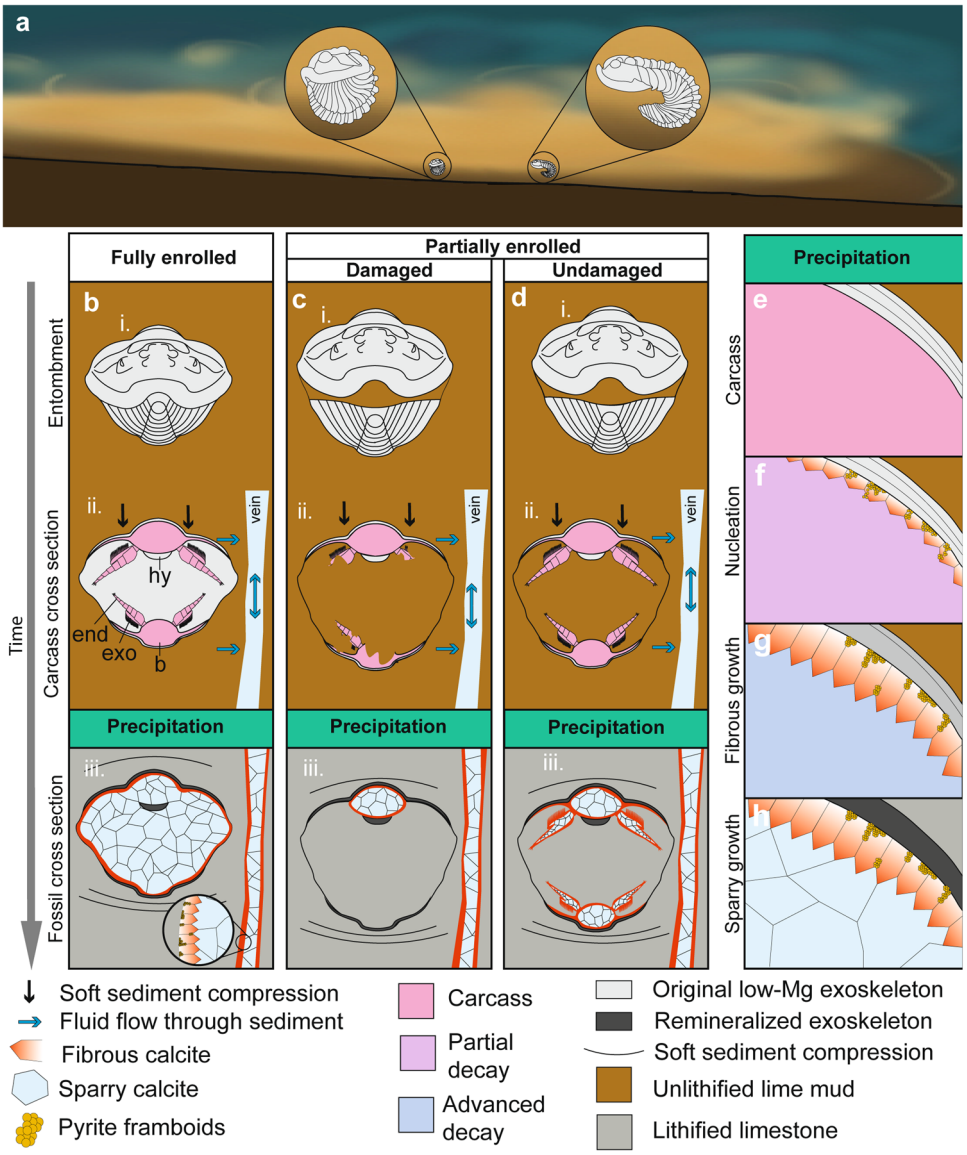

Fig. 6 Taphonomic model for exceptional preservation through calcite replacement in the Walcott-Rust Quarry. a Turbidity flow encases trilobites and entombs them during burial. **b** Fully enrolled pathway. **bi** Frontal view of fully enrolled trilobite entombed. **bii** Cross section of frontal view with no sediment supporting appendages. **biii** Cross section of enrolled specimen filled in by fibrous crust and sparry calcite crystals without preserved appendages. **c** Sediment supported but damaged appendage pathway. **ci** Frontal view of partially enrolled specimen entombed in layer. **cii** Cross section of partially enrolled specimen with appendages damaged by transport in turbidite. **ciii** Cross section of specimen with glabella infilled with calcite and magnification of vein showing pyrite framboids, fibrous and sparry calcite. **d** Sediment supported undamaged appendages. **di** Frontal view of partially enrolled specimen entombed in layer. **dii** Cross section of partially enrolled specimen intact appendages supported by sediment. **diii** Cross section of partially enrolled specimen with appendages preserved in calcite. **e**–**h** Crystal formation. **e** Cross section of undecayed carcass. **f** Early stages of sulfate-reducing bacteria mediated decay with pyrite framboids and magnesium- and iron-bearing fibrous calcite. **g** Advanced microbially mediated decay with continued growth of framboids and fibrous calcite and remineralization of exoskeleton. **h** Sparry calcite precipitation within large void spaces and complete remineralization of exoskeleton.

Decay studies of the caridean shrimp *Crangon crangon* have shown that a single carcass can produce chemical gradients of pH, sulfide, and oxygen into the surrounding substrate[17]. Although this experiment demonstrates that carcass decay will change the composition of the surrounding environment producing a chemical gradient, there is no evidence that the sclerotized exoskeleton functions as an impermeable barrier that would create a drastically different microenvironment within the carcass itself that then led to exceptional preservation. Likewise, although it has been shown that the endogenous bacteria within the digestive system of euarthropods can play an important role in the early diagenetic stabilization of the gut tract due to changes in the pH within the carcass[18], the chemical gradients within the external environment alone are not sufficient to explain the exceptional preservation of other non-biomineralized tissues such as appendages.

Silurian fossils from the Herefordshire Lagersttäte are preserved in concretions that feature a halo with increased aluminum, silicon, iron, and magnesium, as well as depleted calcium[19], suggesting that, in this case, the individual carcasses created chemical gradients within the surrounding matrix. Critically, such elemental halos are entirely absent from the

Walcott-Rust fossils (Figs. 1–3, Supplementary Figs. 3–5), which combined with the lack of concretions, points towards important differences in terms of the lithification of the fossil-bearing strata between these localities. We hypothesize that for the Rust Formation, decay through sulfate-reducing bacteria took place within the carcasses, matrix, and veins as indicated by the presence of pyrite framboids, which may have aided in the precipitation of calcite, but that this process was not restricted to trilobite bodies.

Low iron environment. Previous authors[5] proposed a low iron environment to explain the occurrence of calcite rather than pyrite within trilobite fossils, with the assumption that pyritization would follow a similar microbially-mediated pathway to calcite precipitation. In this work[5] the pyrite observed in the Rust Formation fossils was interpreted as secondary, having replaced the original calcite during late diagenesis (Figs. 2a, 3d, g). In contrast, we demonstrate that pyrite framboids frequently occur around the calcite crystals in both the fossil and veins (Fig. 2a) and embedded within the crystals (Fig. 3d, f, g). Pyrite framboids have been shown to form through the production of hydrogen sulfide by sulfate-reducing bacteria during remineralization of organic matter[20].This suggests that the pyrite framboids within the Rust Formation fossils and veins formed at an early stage, likely mediated by microbial-induced decay, rather than during late diagenesis.

The presence of pyrite throughout the matrix and veins with large volumes of framboids indicates there was more iron within the sediment and pore water than previously suggested[5], but not enough to completely pyritize the carcass as observed in other Ordovician deposits from New York, such as the famous Beecher's Trilobite Bed[21]. Beecher's Bed is located less than 15 miles from the Walcott-Rust Quarry, is similar in age (Late Ordovician), and also formed by turbidity flows, but is a dark shale that experienced extensive exposure to iron-rich pore water, leading to impressively pyritized macrofossils[21]. We hypothesize that fluid flow provided a continuous supply of iron to the veins and allowed for continued pyrite formation during compression and dewatering of the sediment at the Walcott-Rust Quarry, accounting for the large volumes of observed framboids (Fig. 3h–j). In this context, the rigid trilobite exoskeleton prevented internal compaction and vein growth within the carcasses, limiting the amount of available iron and hindering pyritization from sulfate-reducing bacteria within the fossils.

Presence of barite in Rust Formation trilobites. Barium found as rims around clasts in the matrix and large masses of barite within enrolled trilobites have not previously been reported from the Rust Formation. The presence of these features raises questions about the sequence of events leading to the exceptional preservation seen in trilobites (i.e., did the barite precipitate at the same time as calcite or during a later diagenetic event?). Barium is restricted to the external matrix of MCZ:IP:198047, an enrolled specimen found at the surface of Layer 3, suggesting the exoskeleton acted as a barrier to fluid flow after lithification and prevented alteration of the matrix within the specimen (Fig. 3b, d). The specimens with large masses of barite (MCZ:IP:8400 and MCZ:IP:8118) have cracks through which the fluid could have flowed (Fig. 4h). It is unclear if these specimens had original appendage preservation in calcite. In MCZ:IP:8400, the barite mass (light green) runs along the axis of the enrolled specimen with repeated lobe-like structures extending to the pleural lobe (Fig. 4h). It is unclear if this reflects original ventral morphology of the trilobite.

Barite forms in marine sediments when barium- and sulfate-rich waters mix, leading to precipitation[22]. The presence of barite in the Rust Formation implies that nearby barite deposits were dissolved by pore water, creating a barium-rich fluid that flowed through cracks within the lithified or consolidated sediment after the calcite cast fossils had fully formed. This enriched water then flowed between Layers 3 and 4 of the Rust Formation, and through cracks in the rock, such as those seen in MCZ:IP:8400 and MCZ:IP:8118. In some cases, such as the enrolled specimen MCZ:IP:198047, the exoskeleton prevented flow of the enriched water resulting in barium rims around clasts only in the external matrix and not within the fossil.

A new diagenetic model for soft tissue preservation in Rust Formation trilobites. We propose a new model for the exceptional preservation of non-biomineralized structures in the Walcott-Rust trilobites that can be subdivided into three major events: entombment, sediment stabilization, and crystallization (Fig. 6). During the initial entombment stage, turbidity flows transported live trilobites and other organisms such as bryozoans and crinoids (Supplementary Fig. 1d) downslope, ultimately killing them (Fig. 6a). Trilobites enrolled during transport as a defensive mechanism[23–25], with some specimens maintaining complete enrollment after death aided by interlocking co-adaptive devices (Fig. 6a). Depending on the final position during burial, sediment stabilization affected the specimens in different ways. Sediment did not encase the appendages in fully enrolled specimens (Fig. 6bi), and instead produced an empty void following the decay of the soft tissues (Fig. 6bii). In this case, the entire void space filled with calcite crystals without appendage preservation such as specimen MCZ:IP:201000 (Figs. 2a, b, 6biii). By contrast, in partially enrolled specimens the fine-grained sediment encased the non-biomineralized ventral side, including the appendages (Fig. 6c, d). If the appendages were damaged during transportation within the turbidity flow, they were likely destroyed by decay too rapidly before the fine-grained sediment created an external mold (Fig. 6cii). This would result in specimens like MCZ:IP:112030 (Fig. 2f) where calcite is only present in exoskeleton-protected spaces such as the glabella and doublure. In partially enrolled individuals with undamaged appendages, the fine-grained sediment completely encased the non-biomineralized ventral limbs (Fig. 6d). This process created a sediment-supported external mold that preserved exceptional morphological details, including the lamellae and endites, and provided structural protection that prevented collapse or further degradation (Fig. 6dii) such as in specimens MCZ:IP:110933 and MCZ:IP:112018 (Fig. 5a–d).

Regardless of the body position of the trilobites, pyrite framboid and calcite crystal formation started after entombment, and in some instances created an external mold of the appendages (Fig. 6e–h). Oxygen quickly depleted as a result of carcass decay and forced the switch to anoxic pathways, primarily sulfate-reduction through bacteria[26]. Sulfate-reducing decay produced sulfide which combined with iron (II) in the pore water and led to the formation of pyrite framboids (Fig. 6l). Magnesium- and iron-bearing fibrous calcite crystals nucleated off the sediment, encasing the appendages or the exoskeleton, and grew inwards to incorporate framboids into the crystals (Fig. 6l). The originally low magnesium calcite trilobite exoskeleton[8] was at least partially altered during this process, resulting in the observed high magnesium content in the Rust Formation specimens (Fig. 6f–h). Within the fossils, fluid flow limiting available iron (II) concentrations prevented complete pyritization and calcite precipitation dominated. Compression-induced fluid flow carried iron (II) through the veins (Fig. 6bii, cii, dii), facilitating continued pyrite formation within them during calcite precipitation (Fig. 6biii, ciii, diii). While the rigidity of the exoskeleton prevented compaction of the sediment within partially

enrolled specimens and prevented loss of exceptional three-dimensional preservation of the appendages, it also inhibited flow of iron-rich fluid resulting in limited pyrite framboid formation. After the initial phase of fibrous calcite precipitation, large sparry calcite grew within larger void spaces such as the glabella, doublure, and axial lobe of the exoskeleton (Fig. 6biii, ciii, diii), producing various degrees of calcite infilling depending on the extent of the available voids (Fig. 2).

Implications for three-dimensional exceptional fossil preservation. Our findings provide new insights on the mechanisms responsible for the three-dimensional fossilization of non-biomineralized structures through calcite casts, which represents a highly informative but also extremely rare type of exceptional preservation. Calcite casts have been found in diverse conditions, ranging from Ediacaran fossils with crystals replicating the quilt-like body walls[27], and within plant cells[28,29]. However, neither of these cases show evidence of the distinct two phases of calcite precipitation and pyrite framboids as seen in the Walcott-Rust fossils. The only close comparand in the entire Paleozoic is found in the Silurian Herefordshire biota of England, in which diverse organisms (e.g., sponges, euarthropods, mollusks) were encased in a volcaniclastic ash and later incorporated into carbonate concretions[19,30]. Interestingly, both Walcott-Rust and Herefordshire fossils share the same occurrence of pyrite framboids and isopachous rims of fibrous and large sparry calcite crystals despite the different geologic settings (micritic limestones *versus* volcaniclastic sediment with carbonate concretions) and the order of magnitude difference in size of specimens (centimeters *versus* millimeters in width of calcite casts, respectively)[19]. Similarly to the Rust Formation trilobites, Herefordshire fossils also feature pyrite framboids around the margins of calcite infills, which are interpreted as co-precipitating because of their inclusion within calcite crystals[19]. The parallels with the Walcott-Rust Quarry suggest that the pyrite in Herefordshire fossils also formed early during diagenesis as the carcass was decaying and in tandem with calcite growth, rather than at a later stage as previously suggested (*contra* previous authors[5]). However, Herefordshire fossils display a fringe of clay-rich minerals and dolomitization of the concretions[19] that are not observed in the Rust Formation. Herefordshire fossils displays a greater biodiversity with the preservation of entirely soft-bodied organisms such as annelids[31,32] (but see other work[33,34] for alternative interpretations) and aplacophoran mollusks[35]. In these cases, it is likely that the volcaniclastic ash encasing the Herefordshire fossils was more effective at forming an external mold before decay than the micritic sediment. Further comparisons between the two localities are currently underway to better understand the processes responsible for the formation of these exceptional three-dimensional fossils in such different geologic settings.

Exceptional calcite cast preservation is difficult to discover in the field because it is not apparent in hand samples and requires cross sectional examination of large numbers of specimens. Calcite within the doublure of other trilobites is also known in the Silurian *Bumastis*? *phix* from the Dolyhir and Nash Scar Limestone Formation, Dolyhir, UK[36], indicating that similar conditions occurred elsewhere, but to date, appendages with similar preservation have not been found. However, the occurrence of fine-grained sediment flow with enough material to bury but not damage the appendages in a low iron environment is likely not unique to the Walcott-Rust Quarry in the geological record. We hypothesize that exceptional soft-tissue preservation through calcite casts might be more common in the fossil record than currently appreciated, and that the technical difficulties of recognizing it in the field represent the major obstacle in their discovery more broadly.

The calcite cast fossils from the Walcott-Rust Quarry provide a unique view of three-dimensional non-biomineralized trilobite appendages preserved in the original life position with fine detail. Calcite cast fossils, such as those found in Walcott-Rust Quarry and Herefordshire, have preserved delicate detail in three dimensions with little compaction or displacement[5,37] and occur in a variety of geological settings[19]. The spatiotemporally comparable Beecher's Trilobite Bed from New York preserves fully pyritized organisms with comparable levels of morphological detail, including the well-known trilobite *Triarthrus eatoni*; however, non-biomineralized structures such as trilobite limbs are frequently displaced[38]. The Walcott-Rust Quarry provides exceptional external detail comparable to well-known Lagerstätten such as Cambrian Burgess Shale-type sites but with the unique advantage of showing uncompacted appendages within enrolled trilobites, whereas even the three-dimensional fossils from Chengjiang show a degree of post-burial compaction[39–41].

Material and methods

Geological setting. The Spillway Member of the Rust Formation is exposed at the Walcott-Rust Quarry (New York, USA, 43.278533, −75.148761) (Supplementary Fig. 1). The Rust Formation is composed of thinly bedded skeletal wacke and packstones with some heavily bioturbated layers[5]. The quarry itself exposes the "prospect beds" deposited during a highstand, consisting of 14 limestone layers with shale interbeds. Trilobites, bryozoans, cephalopods, and crinoids from the Trenton shelf are frequently found in the quarry within the tempestitic limestone layers, having been deposited by turbidity currents moving from the northwest into a dysoxic foreland basin[5,42]. At the surface of Layer 3, trilobites and crinoids are found both articulated and disarticulated (Supplementary Fig. 1), but only trilobite carcasses show evidence of fossilized non-biomineralized tissues. All specimens prepared as thin sections at the Museum of Comparative Zoology (MCZ) at Harvard University are from Layer 3, which corresponds to a 3–4 cm thick micritic limestone with little bioturbation (Supplementary Fig. 1). Layer 8 has a thickness between 8 and 10 cm, and no trilobites with preserved appendages have been reported to date (Supplementary Fig. 1).

Studied material, imaging, and analyses. Studied specimens of *Ceraurus pleurexanthemus and Flexicalymene senaria* are housed at the Museum of Comparative Zoology, Harvard University. Historic samples were collected from the Walcott-Rust Quarry by Charles Walcott in the 1870s, prepared as thin sections by hand, and affixed to glass slides using balsam sap[6] (Figs. 1, 2). Over 180 kg of rock from Layers 3 and 8 were collected from the Walcott-Rust Quarry based on the presence of trilobites preserved at the surface and donated to the MCZ by Mr. Dan Cooper (Covington, Kentucky, USA) (Supplementary Fig. 1). Three new specimens from Layer 8 (Spillway Member, Rust Formation) were imaged as they showed evidence of calcite within the glabella and doublure (Supplementary Figs. 1, 2). Three trilobite specimens and three calcite veins from Layer 3 (Supplementary Fig. 1) were selected for chemical analyses (Figs. 3a, e, 4a–d) based on the presence of observable sparry calcite either in the hand sample or during grinding of the specimen. The three calcite veins from Layer 3 were chosen to compare minerology with the calcite within fossils to specifically test the hypothesis that enrolled trilobites produced a microenvironment for exceptional preservation[5] (Figs. 3h–j, 4a–d). Veins were frequently found when large slabs (ca. 600 mm across) were broken into smaller pieces (150 to 300 mm across). The veins were selected based on area of calcite exposed and from separate slabs to ensure a broad spatial distribution. Specimens were prepared as one-inch epoxy

mounts. Gold- or palladium/platinum-coated specimens were imaged at Williams College using a ThermoScientific Quattro S scanning electron microscope (SEM) fitted with an Everhart-Thornley, concentric backscatter, and EDAX Octane Elect detectors. Electron dispersive spectroscopy (EDS) spot analyses (30 second dwell) and mapping, and backscattered electron (BSE) and cathodoluminescence (CL) imaging were conducted in a high vacuum environment under 20kv operating conditions. Three-dimensional images of trilobite specimens were obtained using the Bruker SkyScan 1173 micro-CT scanner at the Harvard University Digital Imaging Facility with a voltage of 130 kv, wattage of 61 uA, and 0.25 mm brass filter. Scans were reconstructed as TIFF stacks in NRecon (Bruker Corporation) and visualized in Dragonfly 2019 4.0 (Object Research Systems, Montreal, Canada). Raman spectra were collected at the Center of Nanoscale Systems (CNS) at Harvard University using a Horiba XploRA Plus confocal Raman microscope with a 532 nm laser and 600 grooves/mm diffraction grating and spectral resolution of 1.5 cm^{-1}. Raman spectra were obtained using a 10 s integration time and a 50x Olympus long working distance microscope objective, which focused the beam to a spot size of 1 mm. The spectrometer was calibrated using a silicon wafer to the 520.7 wavenumber Si-Si peak. Two specimens of *Olenoides serratus* from the Burgess Shale (Wuliuan, Cambrian, British Columbia) were photographed for comparative purposes to study the endopodite morphology—one deposited at the Geological Survey of Canada (GSC; Ottawa) and the other at the invertebrate paleontology collections at the Smithsonian Institution (USNM; Washington, D.C., USA). Data was visualized using R. Figures were produced in Adobe Photoshop CS and Adobe Illustrator CS.

Data availability

The data generated and analyzed during this study are available in the Dryad repository, [https://doi.org/10.5061/dryad.1jwstqk16].

Received: 24 April 2023; Accepted: 29 August 2023;
Published online: 19 September 2023

References

1. Walcott, C. D. Notes on *Ceraurus pleurexanthemus*, Green. *Ann. Lyceum Nat. Hist. N. Y.* **11**, 155–159 (1875).
2. Walcott, C. D. Appendages of the Trilobite. *Science* **3**, 279–281 (1884).
3. Raymond, P. E. The appendages, anatomy, and relationships of trilobites. *Mem. Conn. Acad. Arts Sci.* **7**, (1920).
4. Størmer, L. Studies on trilobite morphology. Part I: The thoracic appendages and their phylogenetic significance. *Nor. Geol. Tidsskr.* **19**, 143–274 (1939).
5. Brett, C. E., Whiteley, T. E., Allison, P. A. & Yochelson, E. The Walcott-Rust Quarry: Middle Ordovician Trilobite Konservat-Lagerstätten. *Paleontol. Soc.* **73**, 288–305 (1999).
6. Yochelson, E. L. *Charles Doolittle Walcott, Paleontologist* (The Kent State University Press, 1998).
7. Billings, E. K. Notes on some species of Lower Silurian trilobites. *Q. J. Geol. Soc.* **26**, 479–486 (1870).
8. Wilmot, N. V. Original mineralogy of trilobite exoskeletons. *Palaeontology* **32**, 297–304 (1989).
9. McRoberts, C. A. et al. Original spotted patterns on Middle Devonian phacopid trilobites from western and central New York. *Geology* **41**, 607–610 (2013).
10. Losso, S. R. & Ortega-Hernández, J. Claspers in the mid-Cambrian *Olenoides serratus* indicate horseshoe crab–like mating in trilobites. *Geology* **50**, 897–901 (2022).
11. Walcott, C. D. Cambrian Geology and Paleontology, IV, Appendages of Trilobites. *Smithson. Misc. Collect.* **67**, 115–216 (1918).
12. Bicknell, R. D. C. et al. Biomechanical analyses of Cambrian euarthropod limbs reveal their effectiveness in mastication and durophagy. *Proc. R. Soc. B: Biol. Sci.* **288**, 20202075 (2021).
13. Gabbott, S. E., Xian-guang, H., Norry, M. J. & Siveter, D. J. Preservation of Early Cambrian animals of the Chengjiang biota. *Geology* **32**, 901 (2004).
14. Størmer, L. Studies on trilobite morphology. Part III: The ventral cephalic structures with remarks on the zoological position of the trilobites. *Nor. Geol. Tidsskr.* **29**, 108–158 (1951).
15. Holmes, J. D., Paterson, J. R. & García-Bellido, D. C. The trilobite *Redlichia* from the lower Cambrian Emu Bay Shale Konservat-Lagerstätte of South Australia: systematics, ontogeny and soft-part anatomy. *J. Syst. Palaeontol.* **18**, 295–334 (2020).
16. Bath Enright, O. G., Minter, N. J., Sumner, E. J., Mángano, M. G. & Buatois, L. A. Flume experiments reveal flows in the Burgess Shale can sample and transport organisms across substantial distances. *Commun. Earth Environ.* **2** (2021).
17. Sagemann, J., Bale, S. J., Briggs, D. E. G. & Parkes, R. J. Controls on the formation of authigenic minerals in association with decaying organic matter: an experimental approach. *Geochim. Cosmochim. Acta* **63**, 1083–1095 (1999).
18. Butler, A. D., Cunningham, J. A., Budd, G. E. & Donoghue, P. C. J. Experimental taphonomy of *Artemia* reveals the role of endogenous microbes in mediating decay and fossilization. *Proc. R. Soc. B: Biol. Sci.* **282**, 20150476 (2015).
19. Orr, P. J., Briggs, D. E. G., Siveter, D. J. & Siveter, D. J. Three-dimensional preservation of a non-biomineralized arthropod in concretions in Silurian volcaniclastic rocks from Herefordshire, England. *J. Geol. Soc.* **157**, 173–186 (2000).
20. Mozer, A. A. Authigenic pyrite framboids in sedimentary facies of the Mount Wawel Formation (Eocene), King George Island, West Antarctica. *Pol. Polar Res.* **31**, 255–272 (2010).
21. Farrell, Ú. C., Martin, M. J., Hagadorn, J. W., Whiteley, T. & Briggs, D. E. G. Beyond Beecher's Trilobite Bed: Widespread pyritization of soft tissues in the Late Ordovician Taconic foreland basin. *Geology* **37**, 907–910 (2009).
22. Griffith, E. M. & Paytan, A. Barite in the ocean—occurrence, geochemistry and palaeoceanographic applications. *Sedimentology* **59**, 1817–1835 (2012).
23. Esteve, J., Zamora, S., Gozalo, R. & Liñán, E. Sphaeroidal enrolment in middle Cambrian solenopleuropsine trilobites: Enrolment in Cambrian trilobites. *Lethaia* **43**, 478–493 (2010).
24. Esteve, J., Hughes, N. C. & Zamora, S. Purujosa trilobite assemblage and the evolution of trilobite enrollment. *Geology* **39**, 575–578 (2011).
25. Ortega-Hernández, J., Esteve, J. & Butterfield, N. J. Humble origins for a successful strategy: complete enrolment in early Cambrian olenellid trilobites. *Biol. Lett.* **9**, 20130679 (2013).
26. Froelich, P. N. et al. Early oxidation of organic matter in pelagic sediments of the eastern equatorial Atlantic: suboxic diagenesis. *Geochim. Cosmochim. Acta* **43**, 1075–1090 (1979).
27. Xiao, S., Shen, B., Zhou, C., Xie, G. & Yuan, X. A uniquely preserved Ediacaran fossil with direct evidence for a quilted bodyplan. *Proc. Natl. Acad. Sci.* **102**, 10227–10232 (2005).
28. Retallack, G. J. Scoyenia burrows from Ordovician palaeosols of the Juniata Formation in Pennsylvania. *Palaeontology* **44**, 209–235 (2001).
29. Uhl, D., Jasper, A. & Schweigert, G. Charcoal in the Late Jurassic (Kimmeridgian) of Western and Central Europe—palaeoclimatic and palaeoenvironmental significance. *Palaeobiodiversity Palaeoenvironments* **92**, 329–341 (2012).
30. Siveter, D. J., Briggs, D. E. G., Siveter, D. J. & Sutton, M. D. The Herefordshire Lagerstätte: fleshing out Silurian marine life. *J. Geol. Soc.* https://doi.org/10.1144/jgs2019-110 (2019).
31. Sutton, M. D., Briggs, D. E. G., Siveter, D. J. & Siveter, D. J. A three-dimensionally preserved fossil polychaete worm from the Silurian of Herefordshire, England. *Proc. R. Soc. Lond. B: Biol. Sci.* **268**, 2355–2363 (2001).
32. Struck, T. H., Haug, C., Haszprunar, G., Prpic, N.-M. & Haug, J. T. *Enalikter aphson* is more likely an annelid than an arthropod: a comment to Siveter et al. (2014). *Proc. R. Soc. B: Biol. Sci.* **282**, 20140946 (2015).
33. Siveter, D. J. et al. A Silurian short-great-appendage arthropod. *Proc. R. Soc. B: Biol. Sci.* **281**, 20132986 (2014).
34. Parry, L. A., Legg, D. A. & Sutton, M. D. *Enalikter* is not an annelid: homology, autapomorphies and the interpretation of problematic fossils. *Lethaia* **50**, 222–226 (2017).
35. Sutton, M. D., Briggs, D. E. G., Siveter, D. J. & Siveter, D. J. An exceptionally preserved vermiform mollusc from the Silurian of England. *Nature* **410**, 461–463 (2001).
36. Wilmot, N. V. Primary and diagenetic microstructures in trilobite exoskeletons. *Hist. Biol.* **4**, 51–65 (1990).
37. Siveter, D. J., Fortey, R. A., Briggs, D. E. G., Siveter, D. J. & Sutton, M. D. The first Silurian trilobite with three-dimensionally preserved soft parts reveals novel appendage morphology. *Pap. Palaeontol.* https://doi.org/10.1002/spp2.1401 (2021).
38. Hou, J., Hughes, N. C. & Hopkins, M. J. Gill grooming in middle Cambrian and Late Ordovician trilobites. *Geol. Mag.* 1–6. https://doi.org/10.1017/S001675682300002X (2023).

39. Zhai, D. et al. Three-dimensionally preserved appendages in an early cambrian stem-group pancrustacean. *Curr. Biol.* **29**, 171–177.e1 (2019).
40. Liu, Y., Ortega-Hernández, J., Zhai, D. & Hou, X. A reduced Labrum in a Cambrian Great-Appendage Euarthropod. *Curr. Biol.* **30**, 3057–3061.e2 (2020).
41. Schmidt, M. et al. Before trilobite legs: *Pygmaclypeatus daziensis* reconsidered and the ancestral appendicular organization of Cambrian artiopods. *Philos. Trans. R. Soc. B: Biol. Sci* **377**, 20210030 (2022).
42. Brett, C. E. & Baird, G. C. Revised stratigraphy of the Trenton Group in its type area, central New York State: sedimentology and tectonics of a Middle Ordovician shelf-to-basin succession. *Phys. Chem. Earth Parts ABC* **27**, 231–263 (2002).

Acknowledgements

The authors are deeply grateful to Dan Cooper for generously donating material from the Walcott-Rust Quarry to the MCZ as part of this study; Jessica Cundiff (Museum of Comparative Zoology, Cambridge, USA) and Michelle Coyne (Geological Survey of Canada, Ottawa, Canada) for facilitating specimen access; Phoebe Cohen (Williams College, North Adams MA, USA) for facilitated access to the SEM; Nancy Piatczyc (Williams College, North Adams MA, USA) for assistance with the SEM; Arthur McClelland (Harvard University, Cambridge MA, USA) for assistance collecting Raman spectra. This work is supported by the Palaeontological Association Sylvester-Bradley Award, PA-SB202001 and is published by a grant from the Wetmore Colles fund. The constructive comments of three reviewers helped us improve the manuscript.

Author contributions

S.R.L. and J.O.H. designed the research project. S.R.L. selected specimens for donation and processed material. S.R.L. and J.E.T. prepared specimens for analyses. S.R.L. photographed specimens, collected SEM and Raman data, and produced figures. S.R.L. and J.E.T. analyzed the data. S.R.L. wrote the manuscript with input from J.E.T. and J.O.H. All authors reviewed the final manuscript and gave approval for publication.

Competing interests

The authors declare no competing interests.

Additional information

Supplementary information The online version contains supplementary material available at https://doi.org/10.1038/s43247-023-00981-5.

Correspondence and requests for materials should be addressed to Sarah R. Losso or Javier Ortega-Hernández.

Peer review information *Communications Earth & Environment* thanks the anonymous reviewers for their contribution to the peer review of this work. Primary Handling Editor: Joe Aslin. A peer review file is available.